Formation and Properties of Gels Based on Lipoplexes

ARTICLE *in* THE JOURNAL OF PHYSICAL CHEMISTRY B · MAY 2014

Impact Factor: 3.3 · DOI: 10.1021/jp5023086 · Source: PubMed

3 AUTHORS:

Carlotta Pucci

Sapienza University of Rome

12 PUBLICATIONS **29** CITATIONS

SEE PROFILE

Franco Tardani

Sapienza University of Rome

23 PUBLICATIONS **106** CITATIONS

SEE PROFILE

Camillo La Mesa

Sapienza University of Rome

133 PUBLICATIONS **1,823** CITATIONS

SEE PROFILE

THE JOURNAL OF PHYSICAL CHEMISTRY B

Article

pubs.acs.org/JPCB

Formation and Properties of Gels Based on Lipo-plexes

Carlotta Pucci,[†] Franco Tardani,[†] and Camillo La Mesa*,[†]

[†]Department of Chemistry, Cannizzaro Building, La Sapienza University, P.le A. Moro 5, I-00185 Rome, Italy

ABSTRACT: Aqueous systems containing sodium taurodeoxycholate and, eventually, soybean lecithin were investigated. Depending on the relative amounts of two such species, molecular, micellar, vesicular, liquid crystalline, and solid phases were formed. In the presence of bovine serum albumin, micellar and vesicular systems form lipo-plexes. The latter self-organize into gels, depending on composition and thermal treatments. According to scanning electron microscopy, vesicle-based gels obtained from lipo-plexes form sponge-like entities, whereas micelle-based ones self-arrange in fibrous organizations. Gels are characterized by a significant viscoelasticity in a wide temperature and frequency range. Rheological data were interpreted by assuming strict relations between the system response and the self-organization of the lipo-plexes into gels. It was inferred that differences in the gel properties depend on the different self-assembly modes of the aggregates formed by the mentioned lipo-plexes. Use of the above systems in biomedical applications, mostly in the preparation of matrices requiring the use of smart and biocompatible gels, is suggested.

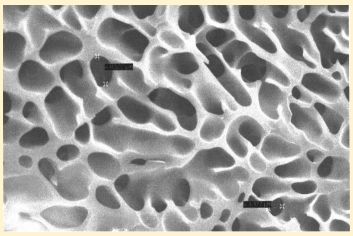

INTRODUCTION

Lipids and/or surfactants self-assemble in water-based media to form micelles, vesicles, and other supra-molecular aggregates. Biopolymer interactions with the above entities give rise to lipo-plexes.[1−5] The mentioned entities are substantiated by a significant stability, biocompatibility, recognition from living tissues,[6] and adsorption onto macroscopic surfaces.[7] In proper concentration regimes, lipo-plexes self-arrange into large domains, forming liquid crystalline or gel phases; the latter are sensitive to stimuli and deformations. The resulting self-organization modes, in fact, control the components mobility,[8] flow properties,[9] and impart significant mechanical and thermodynamic stability to such adducts. This is the rationale underlying the reasons leading to investigate lipo-plexes/based gels. Characterization may help clarify their stability and some macroscopic properties, such as resiliency and elasticity. Given the peculiar features of lipo-plex-based gels, future applications in biomedicine are possible.

The formation of gels based on proteins and their byproducts (collagen, for instance) obtained from mammals and fish is well known.[10,11] Gelation is controlled by concentration, temperature, pH, ionic strength, and combinations thereof.[12] The quality of such gels strongly depends on the preparation procedures, use of acids and/or bases, etc. Their use is essentially focused on the food chemistry field. Their compatibility with tissues is not well-defined, and the same holds for the controlled release of chemicals dispersed therein. For a series of reasons, including the ones mentioned above, their application in the biomedical field has not been adequately investigated for biomedical applications in vivo.

The focus of this work is on gels made by biocompatible surfactants and proteins. Surfactants or lipids may form lipo-plexes upon interaction with proteins; sometimes they do form gels. The above transformation can be rationalized by the sequence: association → interaction with proteins → lipo-plexes formation → coalescence → gelation. The observed sequence is controlled by the phase diagram of the pertinent systems. Therefore, proper mixtures of biological surfactants, lipids, and proteins may originate gels endowed with peculiar micro- and macroscopic properties.

Biocompatible surfactants, such as bile salts, are considered. These species disperse lipids and sterols,[13−15] are present in the bile of mammals, and in the entero-hepatic pool. In addition to their dispersant capacity toward lipids and sterols, bile salts interact with proteins.[16] The phase diagrams and properties of systems containing bile salts have been long known.[17−19] Bile salts form small or cylindrical micelles,[20−23] and liquid crystalline[24−26] and gel phases,[27,28] depending on temperature, concentration, other components, pH, and ionic strength. These are the reasons for investigating the possible formation of lipo-plexes-based gels that contain bile salts. The focus here is on a tauro-derivative of deoxycholic acid, NaTDC, whose properties are not pH-sensitive. In the manipulation of adducts based on the mentioned surfactant it is only required to control the relative amounts of each species, which are necessary to obtain lipo-plexes and gels. These may contain variable amounts of water, NaTDC, bovine serum albumin, BSA, and soybean lecithin, SBL, eventually.

An extensive physicochemical characterization and a precise determination of the pathways leading to gel formation helped to define in detail the properties of above systems. We used rheology, dynamic light scattering (DLS), differential scanning caloimetry (DSC), electrophoretic mobility, NMR self-diffusion, and scanning electron microscopy (SEM) to characterize lipo-plexes and gels formed by the aforementioned species. The former method determined in which temperature, composition, and shear conditions flow and deformation occurs. Rheological investigations found support from electro-

Received: March 6, 2014
Revised: May 14, 2014
Published: May 16, 2014

dx.doi.org/10.1021/jp5023086 | J. Phys. Chem. B 2014, 118, 6107−6116

phoretic mobility, NMR, and light scattering. The meso- and macroscopic organization in the gels was determined by SEM and optical microscopy; the protein state was determined by DSC. Combination of the results based on such investigations gives rise to a self-consistent characterization.

A cogent analysis of the gel structures formed in NaTDC−BSA−(SBL)−water systems offers the opportunity to determine the polymorphic behavior of such complex matrices. The resulting gels are endowed with peculiar properties, making possible their use in formulations. They should be relevant in the preparation of films, covers, and plasters for biomedical applications, such as drug delivery in the entero-hepatic pool.

EXPERIMENTAL SECTION

Materials. Bovine serum albumin, BSA, Sigma-Aldrich, was purified by dialysis and lyophilized. The density, viscosity, pH, and electro-phoretic mobility of its dilute aqueous solutions are equivalent to previously reported values.[29]

High purity sodium taurodeoxycholate, NaTDC, was from Sigma-Aldrich. It was purified by dissolution in hot ethanol, filtered, precipitated by the addition of cold acetone, recovered, and vacuum-dried at 70 °C. Its solution properties (i.e., density, ionic conductivity, and surface tension) are close to available literature data.[13−15]

Soybean L-α-phosphatidylcholine, SBL, Sigma, was purified by standard procedures;[30] its purity was controlled by chromatography. The final product contains essentially C_{16} chains, plus tiny amounts of C_{14} and C_{18} chains (∼1.0 wt % each); no unsaturated fatty acids could be inferred.

Water was doubly distilled in alkaline $KMnO_4$. At 25.0 °C, its ionic conductivity is lower than $1\cdot10^{-7}$ S cm^{-1}. D_2O, of 99.95% isotopic purity, from Aldrich, was used as such.

The organic solvents for the purification procedures, obtained from Sigma-Aldrich, were used as received.

MATERIALS PREPARATION

Binary BSA, NaTDC, and SBL aqueous systems were prepared on a weight percent basis. The above fluids were heated, thermally equilibrated, and mixed with each other in due proportions to form micelles, vesicles, and lipo-plexes (when BSA is present). Proper combination of the components ensured that the optimal concentration required to get lipo-plexes was attained. The individual samples were homogenized by undergoing processes of heating, sonication, vortexing, and centrifugation and were then equilibrated at 25 °C. Equilibration continued until no more changes in the macroscopic phase properties were observed. The control of acidity was not necessary, since NaTDC is a strong electrolyte and BSA acts as a buffer: the pH of the dispersions, in fact, was always in the range 6.2−6.7.

Stable gels were obtained by heating the mentioned lipo-plexes at 40−50 °C. Thermally induced gelation is irreversible. The gels were equilibrated at room temperature for several days, beforethe experiments were performed. Care was taken to keep the gels in vials: in this way, the formation of colloid glasses that occur upon heating and subsequent dehydration was avoided. Liquid crystalline, glasses, or multiphase samples were not considered in what followed. The location of gels in the phase diagrams of the water−NaTDC−BSA and water−NaTDC−BSA−SBL systems is superimposable to what was previously reported.[31,32]

METHODS

Dynamic Light Scattering, DLS. Measurements were run by a Malvern Zeta Nanosizer unit in back scattering mode, at 632.8 nm and 173°. The working temperature was set to 25.0, 40.0, or 50.0 °C. Measurements were run 10 min after introducing the samples in 1.00 cm quartz cells. The latter were cleaned in acid $K_2Cr_2O_7$ and washed with bidistilled water, until the neutrality of the washing fluids was attained. The dispersions passed through 0.22 μm filters before entering the cells. Intensity correlation fits, $I(t)$ vs log t, were elaborated by CONTIN algorithms.[33] The autocorrelation function was derived by

$$g_2(\tau) = \left[\frac{\langle I(t) \times I(t+\tau)\rangle}{\langle I(t)\rangle^2}\right] = 1 + B\,|g_1(t)|^2 \tag{1}$$

where τ (in μs) is the measuring time, and B an instrumental constant. A power expansion in τ analyzed $g_1(\tau)$, according to[34]

$$\ln[g_1(\tau)] = -\Gamma + \left(\frac{\Gamma_2}{2}\right)\tau^2 \tag{2}$$

where Γ_1 and Γ_2 are the first and second cumulant, respectively. Plots of Γ_1 vs q^2 determined the decay of the functions. The decay processes are diffusion-controlled; therefore, the following equality holds

$$D_H = \left[\frac{\Gamma_1}{q^2}\right] \tag{3}$$

where D_H is related to the lipo-plexes diameter through the Stokes−Einstein equation.

Optics. The Tyndall effect was investigated by putting the gels in a homemade metallic box having a narrow glass window. The box is equipped with a camera and a blue light source. Measurements were run in controlled temperature and humidity conditions. Experiments indicate the presence of large scattering domains and deformations due to the application of shear.

ζ-Potential Measurements. The electrophoretic mobility, μ, of colloid entities moving under an applied electric field is proportional to the ζ-potential, ζ, according to[35]

$$\mu = \left[\frac{\varepsilon'\zeta}{4\pi\eta}\right] \tag{4}$$

where η is the solvent viscosity and ε' its static dielectric permittivity. A Malvern laser-Doppler utility measured μ in 3.0 mm U-shaped cells equipped with gold-coated electrodes, at 25.0 °C. The accuracy on ζ-potentials is ±1.0 mV. Each datum is the mean of five independent runs. The solutions were discarded after each set of measurements. Some results are in reported in Figure 3. ζ is related to σ, the surface charge density of lipo-plexes, according to the classical relation

$$\left[\frac{\varepsilon'\zeta}{4\pi}\right] = \left(\frac{\sigma}{\kappa}\right) \tag{4'}$$

where $1/\kappa$ is Debye's screening length. Dimensionally, (σ/κ) is an electric moment per unit area.

NMR Self-Diffusion. Self-diffusion by NMR, D_{NMR} (cm^2 s^{-1}), was determined by pulsed field gradient spin−echo methods, (PFG-SE),[36,37] according to the relation

dx.doi.org/10.1021/jp5023086 | J. Phys. Chem. B 2014, 118, 6107−6116

$$I(2\tau_w, g) = I^\circ \exp\left(-\frac{2\tau_w}{T_2}(g\gamma\delta)^2(\Delta - \frac{\delta}{3}) - D_{NMR}\right) \quad (5)$$

where $I(2\tau_w g)$ is the signal intensity of the selected protons at a field gradient strength equal to g, I° is the unperturbed one, T_2 is the transverse relaxation time, τ_w is the pulse width (usually 100 ms), γ is the gyromagnetic ratio of protons, δ is the pulse duration (in ms), Δ is the repetition time (in ms) and D_{NMR} is the self-diffusion coefficient. High resolution (for protons linked to NaTDC) and low-resolution ones (for bulk water), respectively, were used. In the former case the Bruker WM300 unit worked on ^{1}H at 300.0 MHz. To determine the aggregate self-diffusion, we measured the decay of protons located at 3.25 ppm. Conversely, water self-diffusion, $D_{NMR,wa}$, was determined by a Stelar unit, working at 15.0 MHz on H_2O protons (Table 1). A thermostat controlled the temperature to within ±0.05 °C. A best-fitting procedure based on eq 5 gives values with an uncertainty ∼3% (data not shown). More details on the measuring procedures are reported elsewhere.[38]

Table 1. Water Self-Diffusion in Water−NaTDC−BSA Gels, Left, and Water−NaTDC−BSA−SBL Ones, Right[a]

micelle-based			vesicle-based		
1 − Φ	$D_{NMR,wa}$, 40 °C (10^5 cm^2 s^{-1})	$D_{NMR,wa}$, 50 °C (10^5 cm^2 s^{-1})	1 − Φ	$D_{NMR,wa}$, 40 °C (10^5 cm^2 s^{-1})	$D_{NMR,wa}$, 50 °C (10^5 cm^2 s^{-1})
0.90	2.19	2.55	0.80	1.79	2.11
0.88	2.12	2.47	0.76	1.56	1.74
0.86	2.09	2.46	0.67	1.49	1.62
0.84	2.06	2.40			
0.81	1.99	2.32			
0.80	1.96	2.28			
0.76	1.84	2.14			
0.73	1.75	2.00			

[a] $D_{NMR,wa}$ values are expressed in 10^5 cm^2 s^{-1} units, and refer to different temperatures (in °C), gel structures, and volume fraction in dry matter, (1 − Φ). Errors on $D_{NMR,wa}$ are ±3.0%, those on (1 − Φ) are ±0.005.

Optical Microscopy. A CETI Topic microscope equipped with a Linkam heating stage, working at the required temperature, was used for the optical microscopy measurements. Details on the experimental setup are described elsewhere.[39] The samples were inspected in white light or between crossed Polaroids. Conoscopy was also performed to rule out the presence of liquid crystalline domains.

SEM. Electron microscopy on the gels was performed by a SEM-LEO1450VP unit, equipped with an INCA300 EDS facility. Dispersions were stratified onto accurately cleaned 20 mm × 20 mm glass slides, heated in an oven at 50 °C, and allowed to equilibrate. They were freeze-dried, covered by gold sputtering, and transferred in the SEM chamber. The images were collected and elaborated.

DSC. A Pyris differential scanning calorimeter (Perkin-Elmer) worked under nitrogen gas flow. Measurements were run in the 10−100 °C range at 1.0 °C min^{-1} scan rate, with 2 μW background sensitivity. The BSA denaturation temperature, T_{den} = 72.0 ± 0.1 °C, and the related enthalpy in water, ΔH_{den} (1.84 J g^{-1} of BSA) were used as standards.[40] Errors on ΔH_{den} are lower than ±2.0%.

Rheology. The instrument is a stress-controlled TA AR-1000 unit, working in the 0.1−100 Hz range, in cone−plate geometry and with an electronically controlled rotor position. The plate temperature is constant to ±0.02 °C and is controlled by an external circulating fluid. Details on the apparatus setup are given elsewhere.[41] The gel composition was kept constant and dehydration was avoided by putting wet cotton in an inner aluminum cup located into the measuring chamber. The latter has a hole through which the rotating cone axis is fitted.

Macroscopically homogeneous gels were investigated as a function of applied shear, θ. The optimal θ values were determined in oscillatory conditions, by stress-sweep methods. We selected values ≤5.0 Pa, ensuring the constancy of elastic, G', and viscous, G'', components. The samples were sheared for 1 min before running the experiments. Measurements as a function of frequency, ω, were performed between 0.1 and 100 Hz and analyzed by G' and G'' vs log ω plots. Thermal scans were performed, generally, at 1.0 Hz. Unless otherwise indicated, the thermal scan speed is 1.0 °C min^{-1}. The samples were discarded at the end of each run.

RESULTS

Generalities and Phase Behavior. The characterization of lipo-plexes was preliminarly performed by DLS, Figure 1. From the plot reported therein it is evident that that the size of the mentioned entities is larger than the ones pertinent to both BSA and micelles. The presence of two populations in Figure 1A is ascribed to the coexistence of micelles and lipo-plexes, presumably.

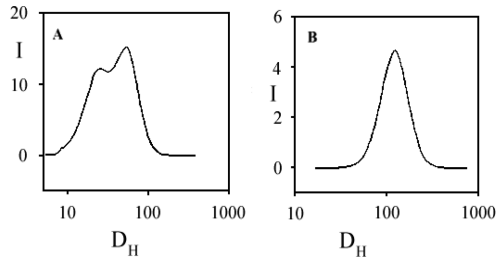

Figure 1. (A) Intensity (in arbitrary units, au) vs D_H (nm) DLS plot for a mixture containing 2.50 wt % NaTDC and 1.30 wt % BSA. (B) Plot for a mixture containing 3.50 wt % NaTDC, 1.50 wt % BSA, and 0.50 wt % SBL. Data were taken at 25.0 °C.

As to vesicle-based lipo-plexes, we noticed that their size is about 30% larger than the one pertinent to the corresponding vesicular entities. Similar conclusions apply to electrophoretic mobility, Figure 2, where a dominant population of entities

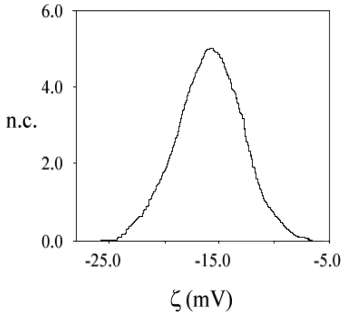

Figure 2. Number of counts, n.c. (10^5), vs ζ-potential, ζ, in mV, for lipo-plexes made of 3.30 wt % NaTDC, 1.30 wt % BSA, and 0.50 wt % SBL, at 25.0 °C.

dx.doi.org/10.1021/jp5023086 | J. Phys. Chem. B 2014, 118, 6107−6116

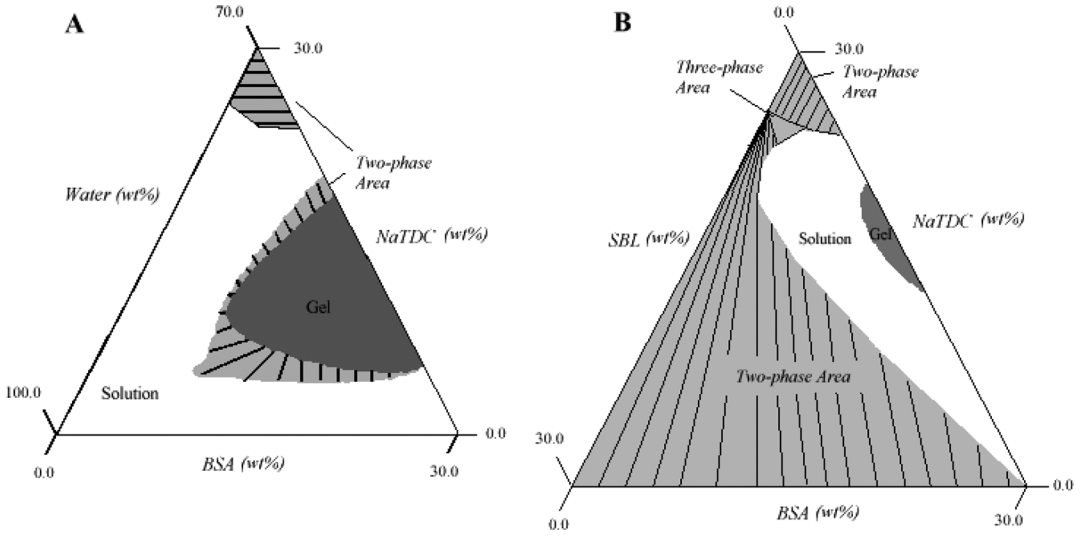

Figure 3. A. Partial phase map of the system water−NaTDC−BSA, at 25 °C. (B) Partial phase map of the system NaTDC−BSA−SBL, at 25 °C and 70.00 wt % water. The two-phase area on the upper corner is a hexagonal/solution region, the one on the bottom is a lamellar/solution one.

moving under the action of the applied electric field is observed. In the ternary systems, conversely, it is presumed that micelles and lipo-plexes coexist when the NaTDB/BSA mole ratio is high.

The partial phase diagrams in Figure 3A,B, indicate the occurrence of solutions, gels, liquid crystalline, and multiphase areas. The phase maps share some features in common with those relative to other water−protein−surfactant systems.[42−44] There are, however, substantial differences too. The phase boundaries shrink on increasing the temperature. This can be an indication that the forces keeping together the lipo-plexes are moderate. In this context, the present protein−surfactant systems behave as weak and thermally modulated gels.

BSA forms lipo-plexes with micelles or vesicles. The electrophoretic mobility of such entities is significantly lower in modulus than that pertinent to free micelles, or vesicles. For instance, the addition of 0.80 wt % BSA to 3.40 wt % NaTDC reduces the ζ-potential from −45 to −18 mV. Similar trends were observed in vesicle-based lipo-plexes. A significant reduction in surface charge density makes easy the nucleation of such entities in gels. When $\zeta < K_BT$, in fact, the barriers avoiding interparticle interactions are reduced, and nucleation is made possible. The effect is significant when $T \geq 40$ °C.

In the following we focus on the lipo-plexes regions observed in the related phase diagrams. Attention was paid to determine the concentrations at which BSA induces the formation of lipo-plexes and gels that are formed upon mild heating of the above entities. The kinetics pathways leading to gelation and the viscoelastic properties of the resulting systems were investigated in some detail.

Macroscopic Gel Properties. Protein−micelle and protein−vesicle lipo-plexes form gels upon heating. At 40 and 50 °C an inverse proportionality between volume fraction of the disperse phase, Φ, and gelation time was observed. Gels are yellowish, transparent, and deformable by application of shear stresses. They are plastic, can be sliced, extruded, and shaped in the form of rods, cups, or disks, are sensitive to humidity, and transform into stiff colloid glasses when strongly dehydrated. Light propagation in the gels indicates significant Tyndall effect, Figure 4; the latter is associated with the presence of large scattering entities.

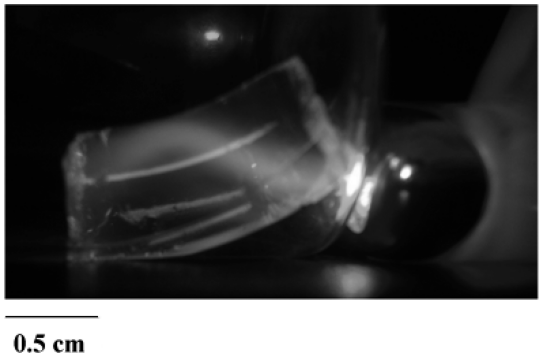

Figure 4. Light propagation in a gel made of 15.2 wt % NaTDC, 12.7 wt % BSA, 2.1 wt % SBL, and water. Halos due to light scattering are observed. The rod size is inferred by comparison with the left-hand side bar.

Freeze-dried gels were investigated by SEM. The presence of different textures was observed; the observed features depend on composition. Micelle-based gels result from the packing into fibrous entities, Figure 5A; vesicle-based ones are sponge-like and form bicontinuous networks with pores in the micrometer range, Figure 5B. It is expected that structurally different gels have a rheological response modulated by the respective packing modes.

At present, it is not known what is the state of BSA in the systems under investigation. It is hardly possible to determine the conformational state of the protein by circular dichroism, because its concentration in the gels, and in lipo-plexes too, is substantial. To ensure that BSA in the gels is somehow related to its native conformation, therefore, DSC experiments were run. The peak ascribed to BSA denaturation, ΔH_{den}, shifts to high temperatures in proportion to the amount of NaTDC and/or SBL in the gels. In all cases, T_{den} of BSA in the gels is >75.0 °C and increases in proportion to NaTDC, or SBL, content. In the range 25.0−50.0 °C, therefore, BSA is not fully denatured. Presumably, however, it is not in its native state.

Kinetics of Gelation. DLS and NMR self-diffusion methods were used. They allow a determination of how fast nucleation is, and to ascertain if gels do form at the end of the sol−gel transition. DLS signals due to the lipo-plexes

dx.doi.org/10.1021/jp5023086 | J. Phys. Chem. B 2014, 118, 6107−6116

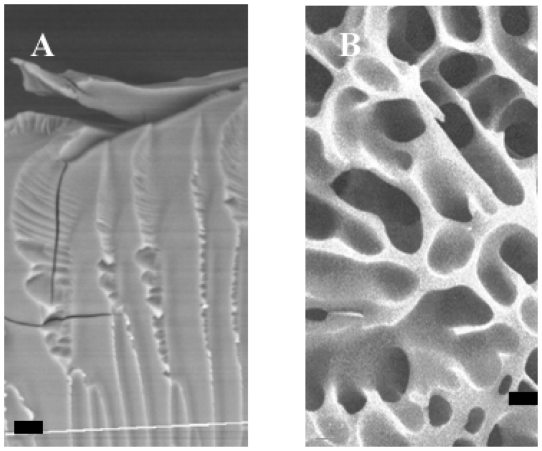

Figure 5. A. SEM image of water-NaTDC-BSA gel having original composition 80.0, 10.5, and 9.50 wt %. Cracks due to partial dehydration can be seen. B. SEM image of a gel originally made of 70.0 water, 14.9 NaTDC, 12.9 BSA, and 2.20 wt % SBL. The sizes of the textures can be inferred by comparison with the bottom bars (0.5 μm for A, and 0.8 μm for B, respectively).

containing BSA are evident at the early stages of the kinetic process. With time, there is a growth in lipo-plexes size, up to complete gelation. Thereafter, D_H values are no longer detected, Figure 6A. To determine the kinetics in concentrated quaternary gels, NMR self-diffusion methods were used, Figure 6B. The trends inferred by NMR share some points in common with those pertinent to DLS. In the following, we assume that the value above which D_H diverge is the gelation time, t_{gel}, Figure 6A. At the onset of gelation, D_{NMR} significantly change in slope, Figure 6B. t_{gel} scales with NaTDC, SBL, BSA concentration, and temperature. An increase in temperature makes coagulation fast; therefore, experiments were run at 40, or 50 °C.

According to electro-phoretic mobility, the repulsive forces between lipo-plexes are reduced by the presence of BSA. As a consequence of an increase in temperature, the kinetics of nucleation speeds up. Nucleation of lipo-plexes leads to the formation of gels; the pathways are weeks long at 25.0 °C, days long at 40 °C, and less at 50.0 °C. In addition to the mentioned effect played by BSA, the time required for gelling significantly decreases with temperature. The kinetic indications given above are qualitative and it is questionable to draw accurate relations between the above quantities. However, the behavior is univocally defined. The process is controlled by BSA concentration. ζ-Potentials in the range |5−20| mV imply moderate surface charge density; this is the reason for an easy nucleation. The barriers avoiding the lipo-plexes collapse are quite lower than the thermal energy (~25−30 mV), and the process is energetically possible. Changes in size during the gelation are controlled by clustering, diffusion, and electro-phoretic mobility terms. In a two-site approximation, the kinetic equations can be expressed as

$$\left(\frac{\partial c_a}{\partial t}\right) + \nabla \times J_a = k_b c_b - k_a c_a \quad (6)$$

$$\left(\frac{\partial c_b}{\partial t}\right) + \nabla \times J_b = k_a c_a - k_b c_b \quad (6')$$

where c_a and c_b are the concentrations of small lipo-plexes, a, or large ones, b. In words, a two-site approximation holds. Equation 6 indicates that nucleation of lipo-plexes is balanced by the respective matter fluxes indicated as J_a and J_b, according to[45]

$$J_a = \mu_a \times \bar{E}_a - D_a \nabla c_a \quad (7)$$

$$J_b = \mu_b \times \bar{E}_b - D_b \nabla c_b \quad (7')$$

The first term in the right-hand side of eq 7 and eq 7′ refers to the electro-phoretic mobility term, when D indicates the self-diffusion. If $\bar{E}$ is zero, eq 7 and eq 7′ reduce to Fick's law. In terms of eqs 6, 6′, 7, and 7′, therefore, the nucleation into large lipo-plexes is diffusion-controlled. Thereafter, gelation takes place.

According to Figure 6 panels A and B, the diffusive processes slow down in proximity of t_{gel}. At constant T, the gelation kinetics is inversely proportional to the volume fraction of the

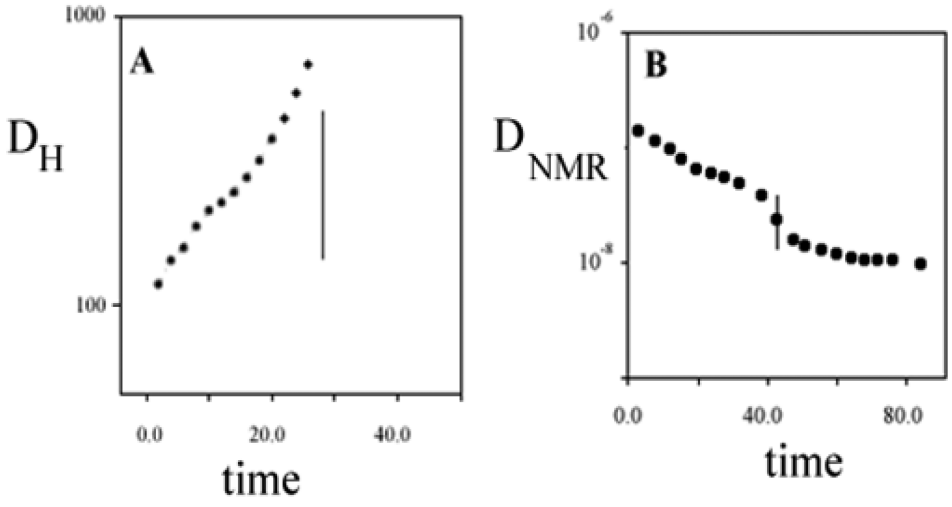

Figure 6. Kinetics of gelation at 50.0 °C. (A) Lipo-plexes size, D_H (in nanometers) vs time (in hours). The gelation time, t_{gel}, is indicated by a vertical bar. The system contains 92.0 wt % water, 4.50 wt % NaTDC, and 3.50 wt % BSA. (B) D_{NMR} ($cm^2\ s^{-1}$) vs time (in hours) for a mixture containing 13.5 wt % NaTDC, 11.8 wt % BSA, 2.00 wt % SBL, and 70.0 wt % D_2O. Two exponential decays occur, before and after t_{gel}, respectively. A tentative gelation time is indicated by a vertical bar.

dx.doi.org/10.1021/jp5023086 | J. Phys. Chem. B 2014, 118, 6107−6116

disperse phase, Φ. When the process goes to completion, D_{NMR} values slow down and D_H ones diverge. The above trends are consistent with general statements on the kinetics of gelation, derived by Shibayama.[46,47] He defined the process in terms of ergodic/non-ergodic approaches and assumed it is concomitant to (1) a significant increase in DLS intensity; (2) a broadening of the related distribution function; (3) the correlation function time becomes $\propto \tau^{-(1-Dp)}$, where D_p has a fractal dimension; (4) a substantial decrease in the slope of the intensity correlation function occurs as $\tau \rightarrow 0$.

The above requirements are fulfilled in all cases reported above.

Visco-elastic Properties. Once gelation is complete, the zero shear viscosity remains constant. We detected whether the latter hypothesis holds in all pertinent cases and chose the conditions suitable for this to occur. Thereafter comparison followed. The rheological properties of micelle-based and vesicle-based gels are significantly different. Links between the rheological behavior and gel structure are, thus, realistic. Presumably, the response is different because of the size and packing modes of the entities that are present in two such media. Fibrous gels, made of BSA and NATDC, flow under shear, whereas the interconnected ones, occurring in the water−BSA−NaTDC−SBL system, do not. In both cases the elastic and viscous contributions are significant and depend on temperature. In the water−NaTDC−BSA system, plots of G' and G'' vs T indicate the crossover of elastic and viscous contributions at the gelation threshold, Figure 7.[48] No such

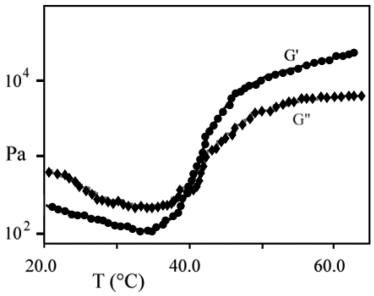

Figure 7. G', circles, and G'', rombuses, in Pa vs temperature, in °C, for a system made of 12.0 wt % BSA and 8.50 NaTDC wt % in water. The thermal gelation threshold is the intersection point of the two curves.

behavior occurs in quaternary systems, Figure 8. The gels, therefore, are structurally different; very presumably, vesicle-based gels arrange in sponge-like entities and show a much higher resistance to shear. A selected visco-elastic spectrum relative to a quaternary system, Figure 9A, indicates a systematic increase of the complex shear viscosity with frequency, and shear-thickening effects. Values as high as 450 Pa are attained at high frequencies. In ternary systems, conversely, values close to 200 Pa are rather common, Figure 9B; they decrease with ω. The differences in the behavior are presumably related to the structural organization in the two gels.

The complex shear viscosity was determined by[49]

$$\eta_s(\omega) = \left(\frac{1}{\omega}\right)\sqrt{(G_s'(\omega)^2) + (G_s''(\omega)^2)} \tag{8}$$

where ω is the applied frequency, in Hz, and

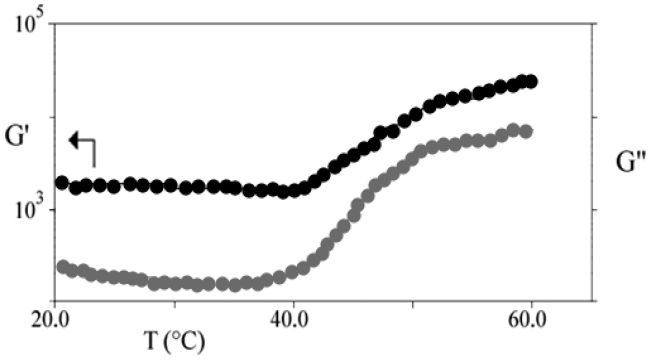

Figure 8. G', full circles, and G'', empty one, in Pa vs temperature, in °C, for a quaternary system containing 13.7 wt % NaTDC, 13.8 wt % BSA, and 2.50 wt % SBL in water. No crossover of G' and G'' curves occurs.

$$G_s' = \sum_{i=1} G_i^\circ\left(\frac{(\omega\tau_i)^2}{1 + (\omega\tau_i)^2}\right) \tag{9}$$

$$G_s'' = \sum_{i=1} G_i^\circ\left(\frac{(\omega\tau_i)}{1 + (\omega\tau_i)^2}\right) \tag{9'}$$

are the real and imaginary components of $\eta_s(\omega)$, respectively. The visco-elasticity of ternary gels decreases with ⌉, Figure 9; the reverse behavior holds in quaternary ones. To get estimates of the visco-elastic relaxation time, the following relation was used[50]

$$\tau_V = \left(\frac{1}{\omega}\right) \times \left(\frac{G'}{G''}\right) \tag{10}$$

where τ_V is the average relaxation time and other symbols are as above. Fits based on eq 10 are constant when a single relaxation process occurs, Figure 10A. In quaternary gels such behavior does not hold, and a Maxwell-like distribution of relaxation times presumably occurs.

Attempts to relate the rheological behavior and the macroscopic gel structure were made. On that purpose approaches formerly developed by Bohlin,[51] and refined by Winter were used.[48] In both cases, the gels are supposed to be formed by the arrangement of different building block units, interacting each with the other during the flow. The limits given by small amplitude oscillations ensure macroscopic stability during the application of shear stresses. Therefore

$$G^* = |G' + jG''| = A\omega^{1/z} \tag{10}$$

where G^* is a frequency-dependent term, modulated by the cooperative energy, A. The G^* term in eq 10 is tuned by a "coordination number", z, related to the number of independent flow units. These are 2 for laminar, 6 for hexagonal, 12 for cubic ones, and so forth.[51] Values close to 6 and 12 were observed in ternary and quaternary gels, respectively. The Maxwell-like distribution of relaxation times that can be evinced by the upper plot in Figure 10A can be related, in our opinion, to a significant connectivity of gel domains.[52] Note that the above behavior is not observed in ternary gels. Therefore, the previous structural hypotheses are experimentally supported.

Lipo-plexes based on micelles or vesicles self-arrange in complex gel structures, held together by BSA. The gels are interconnected and require the application of strong stresses to

dx.doi.org/10.1021/jp5023086 | J. Phys. Chem. B 2014, 118, 6107−6116

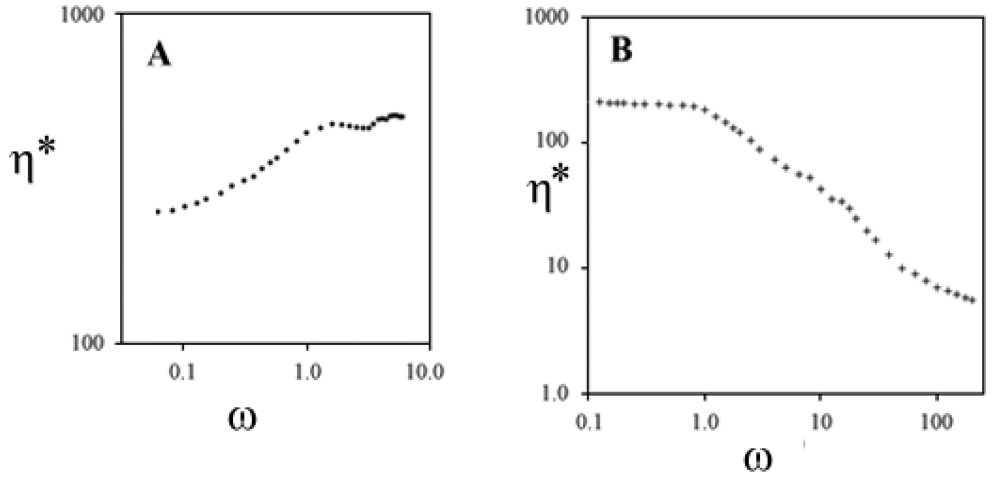

Figure 9. (A) Complex shear viscosity, η^* (Pa), vs ω (Hz), for a quaternary gel containing 14.0 wt % NaTDC, 13.1 wt % BSA and 2.10 wt % SBL in water. (B) The complex shear viscosity of a ternary gel made of 12.0 wt % BSA and 10.0 wt % NaTDC. Data were taken at 25.0 °C. The scale of the left-hand figure is increased.

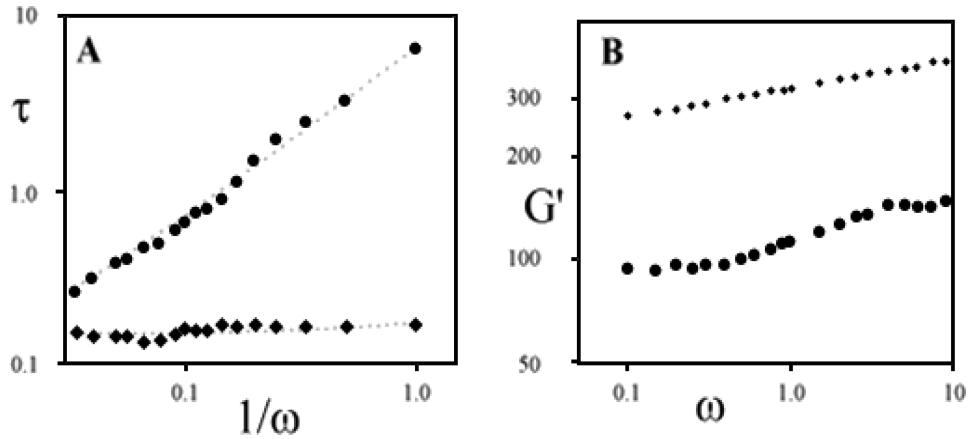

Figure 10. (A) Plot of τ, = $(1/\omega)(G'/G'')$ vs $1/\omega$, at 25.0 °C for ternary, circles, and quaternary gels. Compositions are 13.2 wt % BSA and 11.0 NaTDC wt %; 13.8 wt % NaTDC, 14.2 wt % BSA, and 2.00 wt % SBL for the quaternary, respectively. (B) Plot of G* (Pa) vs ω (Hz) for the same gels.

destroy the organization modes. According to the aforementioned, it is possible to build deformable, or resilient, gels by changing the composition and the type of lipo-plexes from which they are formed.

The local organization is responsible for modifications in the rheological gel properties, mostly in elastic ones. This fact is relevant in the preparation of matrices for the controlled drug release. Detailed investigation could explain why changes in composition and the addition of SBL gives rise to large modifications in macroscopic properties. It would be interesting to detect the concentration thresholds leading to such transitions, and the minimum amount of lipid required for changes to occur. The reported behavior is controlled by the volume fraction of the disperse phase and by the size of the lipo-plexes forming the gels.

■ DISCUSSION

Mixtures of surfactants, lipids, and proteins undergo a wide variety of self-organization modes, with formation of micelles, vesicles, lipo-plexes, liquid crystals, and gels. Gelation is always concomitant to the presence of protein and is assisted by mild thermal treatments. Changes in composition and the presence of lipids imply changes in the gel macroscopic properties, mostly in elasticity. Gel elasticity is common to polymer-based formulations;[53] almost nothing is known on the ones made of lipo-plexes. Protein−surfactant−lipid gels, made up by joining together vesicles, are more elastic than micelle-based ones.

Many papers reported on the formation of lipo-plexes.[54−60] All authors agree that the formation of protein−surfactant complexes is a complicate process, involving several steps, and the combination of electrostatic with hydrophobic effects. In aqueous media the first stage arises from the surfactants uptake in the hydrophobic pockets of the protein, with subsequent conformational changes. At fixed protein content progressive addition of surfactants gives rise to a solution, a multiphase dispersion (at low surfactant/protein mole ratios) and to micelle-mediated redissolution of the precipitates. The phase sequence in the present system is slightly different compared to normal surfactants, because of the rigid steroidal structure of NATDC. Concomitant to the above phase sequence, peculiar effects in the protein state are observed. The denaturation of proteins by surfactants depends on their secondary structure. As a rule, all-β-sheet proteins are less prone to denaturation than α-helical or $\alpha\beta$-mixed ones. This is ascribed to the large number of local contacts in α-helical proteins, allowing their helices to remain intact even after the overall tertiary structure

dx.doi.org/10.1021/jp5023086 | J. Phys. Chem. B 2014, 118, 6107−6116

has been lost, with the helical segments starting to unfold at very high surfactant concentrations. The latter process was demonstrated for the SDS/myoglobin system.[61]

In case of globular proteins, low amounts of surfactant reduce the amount of α-helix in favor of the β-sheet conformation. The former is regained when micelle-assisted redissolution of the complexes takes place and lipo-plexes do form. The tertiary structure of proteins in lipo-plexes is lost at low surfactant content and never recovered. Such evidence suggested the occurrence of a molten globule conformation for proteins in micellar and vesicular media.[62] Very presumably, that conformational state is partly responsible for gelling.

The features reported here have some points in common with what is observed in biological systems. For instance, dedicated studies clarified the rheology of red blood cells, and relations were found between elastic response, particles size, and size-growth, due to the presence of surface-bound proteins.[9] In red blood cells fluids shear deformations help erythrocytes aggregation, with substantial consequences on hemo-rheology. Almost nothing is known on the rheological properties of bile-based gels; that is the reason why we examined the behavior of the latter systems.

It is worth mentioning here that the self-assembly of vesicular entities gives rise to gels endowed with a sponge-like structure. These significantly resist shear stresses, which are uniformly partitioned in the whole gel. This is, in our opinion, the reason why they are characterized by significantly high η^* values and by a relatively poor sensitivity to ω. It is also conceivable, on the same grounds, that gels characterized by a fibrous organization are more sensitive to the shear strength and to the applied frequency, as well. The two organization modes in the gels, therefore, may find use in different applications, both relevant in biomedically oriented formulations.

CONCLUSION

The gels reported here are endowed with peculiar properties. The presence of BSA and moderate thermal treatments are required for gel onset. Gelation is irreversible. At room temperature the gels do not flow under gravity. They can be sliced, shaped to form disks, cups, or rods, and have grossly the same consistency as gelatin-based ones. The above properties are relevant in the formation of gel-based covers and films. Provided they are kept in controlled humidity and temperature conditions, gels remain undisturbed for months. Drying induces a significant reduction in volume and the formation of glassy colloid-based solids.

Modulation in composition leads to different gels, endowed with significant visco-elasticity. Some of those reported here are among the very few cases reported so far where G' is the dominant contribution to visco-elasticity. Gels are characterized by substantial water diffusivity; NMR indicates that self-diffusion is comparable to net water. Presumably, obstruction effects to self-diffusion are present; on such grounds, the gel can be considered continuous, or bicontinuous, depending on the structure and organization modes of the lipo-plexes into gels. The time required for dissolution in water is hours long. For these reasons, gels can be possible drug-release carriers in the intestinal pool.

The most relevant features reported here indicate that changes in composition lead to gels made of building blocks, the lipo-plexes, which pack in different modes. Their self-assembly has consequences on gel consistency, and on the mechanical and transport properties, as well. Similar conditions are met in gels taking part in the formation of cells and tissues. These contain polar lipids, proteins, or collagen. A synergistic combination of the properties inherent to the surfactant, BSA, and lecithin imparts to the resulting materials significant properties, which are not inherent to the single components. In words, the supramolecular organization is responsible for the observed trends. And synergistic effects are relevant. It must be considered, finally, that gels based on lipo-plexes have a substantially higher possibility to disperse lipophilic species compared to protein based ones.

Tuning the phase properties has consequences in formulation, when the preparation of "ad hoc" materials is required. More detailed information and dedicated studies on the relations between macroscopic structure, organization modes, protein conformation, surfactant or lipid nature, overall composition, and rheological performances of such gels could be helpful. Further investigation could give the opportunity to prepare biocompatible matrices replacing, or implementing, previously existing ones.

AUTHOR INFORMATION

Corresponding Author

*E-mail: camillo.lamesa@uniroma1.it.

Notes

The authors declare no competing financial interest.

ACKNOWLEDGMENTS

The Ministry of Education and Scientific Research supported the present project through a PRIN on polymer−surfactants systems.

REFERENCES

(1) Chen, S. H. Structure and fractal dimension of protein-detergent complexes. *Phys. Rev. Lett.* **1986**, *57*, 2583−2586.

(2) Turro, N. J.; Lei, X.-G.; Ananthapadmanabhan, K. P.; Aronson, M. Spectroscopic probe analysis of protein-surfactant interactions: The BSA/SDS System. *Langmuir* **1995**, *11*, 2525−2533.

(3) Valstar, A.; Brown, W.; Almgren, M. The lysozyme-sodium dodecyl sulfate system studied by dynamic and static light scattering. *Langmuir* **1999**, *15*, 2366−2374.

(4) Valstar, A.; Vasilescu, M.; Vigouroux, C.; Stilbs, P.; Almgren, M. Heat-set bovine serum albumin-sodium dodecyl sulfate gels studied by fluorescence probe methods, NMR, and light scattering. *Langmuir* **2001**, *17*, 3208−3215.

(5) Andreozzi, P.; Bonincontro, A.; La Mesa, C. Electrostatic interactions between a protein and oppositely charged micelles. *J. Phys. Chem. B* **2008**, *112*, 3339−3345.

(6) (a) Steele, J. G.; Dalton, B. A.; Johnson, G.; Underwood, P. A. Adsorption of fibronectin and vitronectin onto Primaria and tissue culture polystyrene and relationship to the mechanism of initial attachment of human vein endothelial cells and BHK-21 fibroblasts. *Biomaterials* **1995**, *16*, 1057−1067. (b) Wittmer, C. R.; Phelps, J. A.; Saltzman, W. M.; Van Tassel, P. R. Fibronectin terminated multilayer films: Protein adsorption and cell attachment studies. *Biomaterials* **2006**, *28*, 851−860. (c) Stebelska, K.; Dubielecka, P. M.; Sikorski, A. F. The effect of phosphatidylserine content on the ability of natural membranes to fuse with positively charged liposomes and lipo-plexes. *J. Membr. Biol.* **2006**, *206*, 203−214.

(7) Bogatu, B.; Contag, B. Adsorption of lipoproteins onto mineral dust surfaces: A possible factor in the pathogenesis of particle-induced pulmonary fibrosis? *Zeit. Naturforsch. C* **2005**, *60*, 792−798.

(8) (a) Reitan, N. K.; Juthajan, A.; Lindmo, T.; de Lange, D. C. Macromolecular diffusion in the extracellular matrix measured by fluorescence correlation spectroscopy. *J. Biomed. Optics* **2008**, *13*, 054040/1−9. (b) Brohede, U.; Bramer, T.; Edsman, K.; Stromme, M.

Electrodynamic Investigations of Ion Transport and Structural Properties in Drug-Containing Gels: Dielectric Spectroscopy and Transient Current Measurements on Catanionic Carbopol Systems. *J. Phys. Chem. B* **2005**, *109*, 15250−15255.
(9) (a) Thurston, G. B.; Gaertner, E. B. Viscoelasticity of electrorheological fluids during oscillatory flow in a rectangular channel. *J. Rheol. (N.Y.)* **1991**, *35*, 1327−1343. (b) Ulker, P.; Sati, L.; Celik-Ozenci, C.; Meiselman, H. J.; Baskurt, O. K. Mechanical stimulation of nitric oxide synthesizing mechanisms in erythrocytes. *Biorheology* **2009**, *46*, 121−132. (c) Bosman, G.J.C.G.M. Erythrocyte ageing in vivo and in vitro: structural aspects and implications for transfusion. *Transfus. Med.* **2008**, *18*, 335−347.
(10) Chen, J.; Dickinson, E.; Lee, H. S.; Lee, W. P. Protein-based emulsion gels; Effects of interfacial properties temperature. *Special Publ. R. Soc. Chem.* **2001**, *258* (Food Colloids), 384−391.
(11) Mleko, S.; Tomczynska-Mleko, M.; Targonski, Z. Globular protein gels as carriers of active substances. *Agro Food Industry Hi-Tech* **2010**, *21*, 26−68.
(12) Oztop, M. H.; Rosenberg, M.; Rosenberg, Y.; McCarhy, K. L.; McCarthy, M. J. Magnetic resonance imaging (MRI) and relaxation spectrum analysis as methods to investigate swelling in whey protein gels. *J. Food Sci.* **2010**, *75*, E508−E515.
(13) Donovan, J. M.; Jackson, A. A.; Carey, M. C. Molecular species composition of inter-mixed micellar/vesicular bile salt concentrations in model bile: dependence upon hydrophilic-hydrophobic balance. *J. Lipid Res.* **1993**, *34*, 1131−1140.
(14) (a) Hofmann, A. F.; Mysels, K. J. Bile acid solubility and precipitation in vitro and in vivo: The role of conjugation, pH, and calcium ions. *J. Lipid Res.* **1992**, *33*, 617−626. (b) Hjelm, R. P.; Schteingart, C. D.; Hofmann, A. F.; Thiyagarajan, P. Structure of conjugated bile salt−fatty acid−monoglyceride mixed colloids: Studies by small-angle neutron scattering. *J. Phys. Chem. B* **2000**, *104*, 197−211.
(15) Redinger, R. N.; Small, D. M. Bile composition, bile salt metabolism, and gallstones. *Arch. Int. Med.* **1972**, *130*, 618−630.
(16) Leggio, C.; Galantini, L.; Zaccarelli, E.; Pavel, N. V. Small-angle X-ray scattering and light scattering on lysozyme and sodium glycocholate micelles. *J. Phys. Chem. B* **2005**, *109*, 23857−23869.
(17) Small, D. M. Liquid crystals in living and dying systems. *J. Colloid Interface Sci.* **1977**, *58*, 581−602.
(18) (a) Small, D. M.; Bourges, M.; Dervichian, D. G. Ternary and quaternary aqueous systems containing bile salt, lecithin, and cholesterol. *Nature* **1966**, *211*, 816−818. (b) Small, D. M.; Bourges, M.; Dervichian, D. G. The biophysics of lipidic associations. I. The ternary systems lecithin−bile salt−water. *Biochim. Biophys. Acta* **1966**, *125*, 563−580. (c) Bourges, M.; Small, D. M.; Dervichian, D. G. Biophysics of lipid associations. III. Quaternary systems lecithin−bile salt−cholesterol−water. *Biochim. Biophys. Acta* **1967**, *144*, 189−201.
(19) Ulmius, J.; Lindblom, G.; Wennerström, H.; Johansson, L.B.-Å; Fontell, K.; Söderman, O.; Arvidson, G. Molecular organization in the liquid-crystalline phases of lecithin-sodium cholate-water systems studied by nuclear magnetic resonance. *Biochemistry* **1982**, *21*, 1553−1560.
(20) Mazer, N. A.; Carey, M. C.; Kwasnick, R. F.; Benedek, G. B. Quasielastic light scattering studies of aqueous biliary lipid systems. Size, shape, and thermodynamics of bile salt micelles. *Biochemistry* **1979**, *18*, 3064−3075.
(21) Briganti, G.; D'Archivio, A. A.; Galantini, L.; Giglio, E. Structural study of the micellar aggregates of sodium and rubidium glyco- and taurodeoxycholate. *Langmuir* **1996**, *12*, 1180−1187.
(22) D'Archivio, A. A.; Galantini, L.; Giglio, E.; Jover, A. X-ray and quasi-elastic light-scattering studies of sodium deoxycholate. *Langmuir* **1998**, *14*, 4776−4781.
(23) (a) Galantini, L.; Giglio, E.; La Mesa, C.; Pavel, N. V.; Punzo, F. Sodium taurodeoxycholate structure from solid to liquid phase. *Langmuir* **2002**, *18*, 2812−2816. (b) La Mesa, C. A. Supra-molecular association in bile salts. *Recent Res. Dev. Surf. Colloids* **2004**, *1*, 97−115.
(24) Edlund, H.; Khan, A.; La Mesa, C. Formation of a liquid crystalline phase in the water-sodium taurodeoxycholate system. *Langmuir* **1998**, *14*, 3691−3697.
(25) Marques, E. F.; Edlund, H.; La Mesa, C.; Khan, A. Liquid crystals and phase equilibria: Binary bile salt-water systems. *Langmuir* **2000**, *16*, 5178−5186.
(26) Amenitsch, H.; Edlund, H.; Khan, A.; Marques, E. F.; La Mesa, C. Bile salts form lyotropic liquid crystals. *Colloids Surf., A* **2003**, *213*, 79−92.
(27) Rich, A.; Blow, D. M. Formation of a helical steroid complex. *Nature* **1958**, *182*, 423−426.
(28) Youssry, M.; Coppola, L.; Furia, E.; Oliviero, C.; Nicotera, I. A new physicochemical characterization of sodium taurodeoxycholate/water system. *Phys. Chem. Chem. Phys.* **2008**, *10*, 6880−6889.
(29) Monkos, K. On the hydrodynamics and temperature dependence of the solution conformation of human serum albumin from viscometry approach. *Biochim. Biophys. Acta* **2004**, *1700*, 27−34.
(30) Camusso, C.; Maroto, B. Hydrophobic interactions in the purification of soybean lecithin. *J. Am. Oil Chem. Soc.* **1995**, *72*, 613−615.
(31) Orioni, B.; Roversi, M.; La Mesa, C.; Asaro, F.; Pellizer, G.; D'Errico, G. Polymorphic behavior in protein-surfactant mixtures: The water−bovine serum albumin−sodium taurodeoxycholate system. *J. Phys. Chem. B* **2006**, *110*, 12129−12140.
(32) Calabresi, M.; Andreozzi, P.; La Mesa, C. Supramolecular association and polymorphic behaviour in systems containing bile acid salts. *Molecules* **2007**, *12*, 1731−1754.
(33) Koppel, D. E. Analysis of macromolecular polydispersity in intensity correlation spectroscopy. Method of cumulants. *J. Chem. Phys.* **1972**, *57*, 4814−4820.
(34) Sallustio, S.; Galantini, L.; Gente, G.; Masci, G.; La Mesa, C. Hydrophobically modified pullulans: Characterization and physicochemical properties. *J. Phys. Chem. B* **2004**, *108*, 18876−18883.
(35) Adamson, A. W. *Physical Chemistry of Surfaces*, 5th ed.; Wiley: New York, 1991; Chapter V, p 218.
(36) Stilbs, P. Fourier transform pulsed-gradient spin-echo studies of molecular diffusion. *Progr. NMR Spectrosc.* **1987**, *19*, 1−45.
(37) Chidichimo, G.; La Mesa, C.; Ranieri, G. A.; Terenzi, M. NMR investigation of the lamellar mesophase occurring in the system aerosol OT-water. Mol. Cryst. *Liq. Cryst.* **1987**, *150b*, 221−236.
(38) Gente, G.; La Mesa, C.; Muzzalupo, R.; Ranieri, G. A. Micelle formation and phase equilibria in a water−trifluoroethanol−fluorocarbon surfactant system. *Langmuir* **2000**, *16*, 7914−7919.
(39) Bonicelli, M. G.; Ceccaroni, G. F.; La Mesa, C. Lyotropic and thermotropic behavior of alkylglucosides and related compounds. *Colloid Polym. Sci.* **1998**, *276*, 109−116.
(40) Boye, J. J.; Inteaz, A.; Ismail, A. A. Interactions involved in the gelation of bovine serum albumin. *J. Agric. Food Chem.* **1996**, *44*, 996−1004.
(41) Roversi, M.; La Mesa, C. Rheological properties of protein-surfactant based gels. *J. Colloid Interface Sci.* **2005**, *284*, 470−476.
(42) Morèn, A. K.; Khan, A. Phase equilibria of an anionic surfactant (sodium dodecyl sulfate) and an oppositely charged protein (lysozyme) in water. *Langmuir* **1995**, *11*, 3636−3643.
(43) Morèn, A. K.; Khan, A. Surfactant hydrophobic effect on the phase behavior of oppositely charged protein and surfactant mixtures: Lysozyme and sodium alkyl sulfates. *Langmuir* **1998**, *14*, 6818−6826.
(44) Sesta, B.; Gente, G.; Iovino, A.; Laureti, F.; Michiotti, P.; Paiusco, O.; Palacios, A. C.; Persi, L.; Princi, A.; Sallustio, S.; Sarnthein-Graf, C.; Capalbi, A.; La Mesa, C. Supramolecular association in the system water−lysozyme−lithium perfluorononanoate. *J. Phys. Chem. B* **2004**, *108*, 3036−3043.
(45) Berne, B. J.; Pecora, R. *Dynamic Light Scattering, with Applications to Chemistry, Biology and Physics*; Wiley & Sons: New York, 1976; Chapter VI, p 92.
(46) Matsunaga, T.; Shibayama, M. Gel point determination of gelatin hydrogels by dynamic light scattering and rheological measurements. *Phys. Rev. E* **2007**, *76*, 030401/1−030401/4.

(47) Okamoto, M.; Norisuye, T.; Shibayama, M. Time-resolved dynamic light scattering study on gelation and gel-melting processes of gelatin gels. *Macromolecules* **2001**, *34*, 8496−8502.
(48) Winter, H. H. Can the gel point of a crosslinking polymer be detected by the $G'-G''$ crossover? *Polym. Eng. Sci.* **1987**, *27*, 1698−1702.
(49) Macosko, C. W. *Rheology: Principles, Measurements and Applications*; VCH: New York, 1993; Chapter III, p 109.
(50) (a) Rehage, H.; Hoffmann, H. Viscoelastic surfactant solutions: Model systems for rheological research. *Mol. Phys.* **1991**, *74*, 933−973. (b) Kilpatrick, P. K.; Khan, S. A.; Tayal, A.; Blackburn, J. C. In *Structure and Flow in Surfactant Solutions*; Herb, C. A., Prud'Homme, R. K., Eds.; American Chemical Society: Washington, DC, 1994; p 229.
(51) Bohlin, L. A theory of flow as a cooperative phenomenon. *J. Colloid Interface Sci.* **1980**, *74*, 423−434.
(52) Ferry, J. D. *Viscoelastic Properties of Polymers*; Wiley: New York, 1980.
(53) Cellesi, F.; Weber, W.; Fussenegger, M.; Hubbell, J. A.; Tirelli, N. Towards a fully synthetic substitute of alginate: Optimization of a thermal gelation/chemical cross-linking scheme ("tandem" gelation) for the production of beads and liquid-core capsules. *Biotechnol. Bioeng.* **2004**, *88*, 740−749.
(54) Reynolds, J. A.; Tanford, C. Gross conformation of protein-sodium dodecylsulfate complexes. *J. Biol. Chem.* **1970**, *245*, 5166−5168.
(55) Turro, N. J.; Lei, L. S.; Ananthapadmanabhan, K. P.; Aronson, M. Spectroscopic probe analysis of protein−surfactant interactions: The BSA/SDS System. *Langmuir* **1995**, *11*, 2525−2533.
(56) Valstar, A.; Vasiliescu, M.; Vigorous, C.; Stilbs, P.; Almgren, M. Heat-set bovine serum albumin-sodium dodecylsulfate gels studied by fluorescence probe methods, NMR and light scattering. *Langmuir* **2001**, *17*, 3208−3215.
(57) Jones, M. N.; Manley, P. Interaction between lysozyme and *n*-alkyl sulphates in aqueous solution. *J. Chem. Soc. Faraday Trans. I* **1980**, *76*, 654−664.
(58) Chen, S. H.; Teixeira, J. Structure and fractal dimension of protein-detergent Complexes. *Phys. Rev. Lett.* **1986**, *57*, 2583−2586.
(59) Stenstam, A.; Khan, A.; Wennerstrom, H. The lysozyme-dodecyl sulfate system. An example of protein-surfactant aggregation. *Langmuir* **2001**, *17*, 7513−7520.
(60) Goddard, E. D.; Ananthapadmanabhan, K. P. *Interactions of Surfactants with Polymers and Proteins*; CRC Press: Boca Raton, 1993. See, in particular, Chapter VIII, 319−365.
(61) Andersen, K. K.; Westh, P.; Otzen, D. E. Global study of myoglobin-surfactant interactions. *Langmuir* **2008**, *24*, 399−407.
(62) Agarraberes, F. A.; Dice, J. F. Protein translocation across membrane. *Biochim. Biophys. Acta, Biomembr.* **2001**, *1513*, 1−24.